Free vibration of axially loaded thin-walled composite box beams

Thuc Phuong Vo* and Jaehong Lee†

Department of Architectural Engineering, Sejong University
98 Kunja Dong, Kwangjin Ku, Seoul 143-747, Korea

(Dated: March 12, 2009)

A general analytical model applicable to flexural-torsional coupled vibration of thin-walled composite box beams with arbitrary lay-ups under a constant axial force has been presented. This model is based on the classical lamination theory and accounts for all the structural coupling coming from the material anisotropy. Equations of motion are derived from the Hamilton's principle. A displacement-based one-dimensional finite element model is developed to solve the problem. Numerical results are obtained for thin-walled composite box beams to investigate the effects of axial force, fiber orientation and modulus ratio on the natural frequencies, load-frequency interaction curves and corresponding vibration mode shapes.

Keywords: Thin-walled composite beam; classical lamination theory; flexural-torsional coupled vibration; axial force

I. INTRODUCTION

Fiber-reinforced composite materials have been used over the past few decades in a variety of structures. Composites have many desirable characteristics, such as high ratio of stiffness and strength to weight, corrosion resistance and magnetic transparency. Thin-walled structural shapes made up of composite materials, which are usually produced by pultrusion, are being increasingly used in many engineering fields. However, the structural behavior is very complex due to coupling effects as well as warping-torsion and therefore, the accurate prediction of stability limit state and dynamic characteristics is of the fundamental importance in the design of composite structures.

The theory of thin-walled members made of isotropic materials was first developed by Vlasov [1] and Gjelsvik [2]. Up to the present, investigation into the stability and vibrational behavior of these members has received widespread attention and has been carried out extensively. Closed-form solution for flexural and torsional natural frequencies, critical buckling loads of isotropic thin-walled bars are found in the literature (Timoshenko [3,4] and Trahair [5]). For some practical applications, earlier studies have shown that the effect of axial force on the natural frequencies and

*Graduate student

†Professor, corresponding author. Tel.:+82-2-3408-3287; fax:+82-2-3408-3331

; Electronic address: jhlee@sejong.ac.kr

mode shapes is more pronounced than those of the shear deformation and rotary inertia. Although a large number of studies has been performed on the dynamic characteristics of axially loaded isotropic thin-walled beams, it should be noted that only a few deal with thin-walled composite structures with arbitrary lay-ups. A literature survey on the subject shows that there appears some works reported on the free vibration of axially loaded closed-section thin-walled composite beams. Many numerical techniques have been used to solve the dynamic analysis of these members. One of the most effective approach is to derive the exact stiffness matrices based on the solution of the differential equation of beam. Most of those studies adopted an analytical method that required explicit expressions of exact displacement functions for governing equations. Banerjee [6,7] applied the exact dynamic stiffness matrix to perform the free vibration analysis of axially loaded composite Timoshenko beams. The works of Li et al. [8-11] deserved special attention because they developed the analytical solution to determine the flexure-torsion coupled dynamic responses of axially loaded thin-walled composite beam under concentrated, distributed time-dependent loads and external stochastic excitations. The influences of axial force, Poisson effect, axial deformation, shear deformation and rotary inertia were discussed in their research. Kaya and Ozgumus [12] introduced the differential transform method (DTM) to analyse the free vibration response of an axially loaded, closed-section composite Timoshenko beam which featured material coupling between flapwise bending and torsional vibrations. The effects of the bending-torsion coupling, the axial force and the slenderness ratio on the natural frequencies were inspected. In the research of Banerjee and Li et al. and Kaya and Ozgumus [6-12], it was very effective in saving the computing time due to the closed-form solution which can be easily derived by the help of symbolic computation. However, the analytical operations were often too complex to yield exact displacement functions in the case of solving a system of simultaneous ordinary differential equations with many variables. Additionally, they considered only a cantilever glass-epoxy composite beam with rectangular cross section in the numerical examples. By using finite element method, Bank and Kao [13] analysed free and forced vibration of thin-walled fibre reinforced composite material beams by using the Timoshenko beam theory. Song et al. [14] carried out the vibration and stability of pretwisted spinning thin-walled composite beams featuring bending-bending elastic coupling. Recently, Cortinez, Machado and Piovan [15,16] presented a theoretical model for the dynamic analysis of thin-walled composite beams with initial stresses. Machado et al. [17] determined the regions of dynamic instability of simply supported thin-walled composite beam subjected to an axial excitation. The analysis was based on a small strain and moderate rotation theory, which was formulated through the adoption of a second-order displacement field. In their research [15-17], thin-walled composite beams for both open and closed cross-sections and the shear flexibility (bending, non-uniform warping) were incorporated. However, it was strictly valid

for symmetric balanced laminates and especially orthotropic laminates. By using using a boundary element method, Sapountzakis and Tsiatas [18] solved the general flexural-torsional buckling and vibration problems of composite Euler-Bernoulli beams of arbitrarily shaped cross section. This method overcame the shortcoming of possible thin tube theory solution, which its utilization had been proven to be prohibitive even in thin-walled homogeneous sections.

In this paper, which is an extension of the authors' previous works [19-21], flexural-torsional coupled vibration of thin-walled composite box beams with arbitrary lay-ups under a constant axial force is presented. This model is based on the classical lamination theory, and accounts for all the structural coupling coming from the material anisotropy. Equations of motion are derived from the Hamilton's principle. A displacement-based one-dimensional finite element model is developed to solve the problem. Numerical results are obtained for thin-walled composite box beams to investigate the effects of axial force, fiber orientation and modulus ratio on the natural frequencies, load-frequency interaction curves and corresponding vibration mode shapes.

II. KINEMATICS

The theoretical developments presented in this paper require two sets of coordinate systems which are mutually interrelated. The first coordinate system is the orthogonal Cartesian coordinate system (x, y, z), for which the x and y axes lie in the plane of the cross section and the z axis parallel to the longitudinal axis of the beam. The second coordinate system is the local plate coordinate (n, s, z) as shown in Fig.1, wherein the n axis is normal to the middle surface of a plate element, the s axis is tangent to the middle surface and is directed along the contour line of the cross section. The (n, s, z) and (x, y, z) coordinate systems are related through an angle of orientation θ as defined in Fig.1. Point P is called the pole axis, through which the axis parallel to the z axis is called the pole axis.

To derive the analytical model for a thin-walled composite beam, the following assumptions are made:

1. The contour of the thin wall does not deform in its own plane.
2. The linear shear strain $\bar{\gamma}_{sz}$ of the middle surface is to have the same distribution in the contour direction as it does in the St. Venant torsion in each element.
3. The Kirchhoff-Love assumption in classical plate theory remains valid for laminated composite thin-walled beams.
4. Each laminate is thin and perfectly bonded.
5. Local buckling is not considered.

According to assumption 1, the midsurface displacement components $\bar{u}, \bar{v}$ at a point A in the contour coordinate system can be expressed in terms of a displacements U, V of the pole P in the x, y directions, respectively, and the rotation angle Φ about the pole axis,

$$\bar{u}(s,z) = U(z)\sin\theta(s) - V(z)\cos\theta(s) - \Phi(z)q(s) \tag{1a}$$

$$\bar{v}(s,z) = U(z)\cos\theta(s) + V(z)\sin\theta(s) + \Phi(z)r(s) \tag{1b}$$

These equations apply to the whole contour. The out-of-plane shell displacement $\bar{w}$ can now be found from the assumption 2. For each element of middle surface, the shear strain become

$$\bar{\gamma}_{sz} = \frac{\partial\bar{v}}{\partial z} + \frac{\partial\bar{w}}{\partial s} = \Phi'(z)\frac{F(s)}{t(s)} \tag{2}$$

where $t(s)$ is thickness of contour box section, $F(s)$ is the St. Venant circuit shear flow.

After substituting for $\bar{v}$ from Eq.(1) and considering the following geometric relations,

$$dx = ds\cos\theta \tag{3a}$$

$$dy = ds\sin\theta \tag{3b}$$

Eq.(2) can be integrated with respect to s from the origin to an arbitrary point on the contour,

$$\bar{w}(s,z) = W(z) - U'(z)x(s) - V'(z)y(s) - \Phi'(z)\omega(s) \tag{4}$$

where differentiation with respect to the axial coordinate z is denoted by primes ($'$); W represents the average axial displacement of the beam in the z direction; x and y are the coordinates of the contour in the (x, y, z) coordinate system; and ω is the so-called sectorial coordinate or warping function given by

$$\omega(s) = \int_{s_\circ}^{s}\Big[r(s) - \frac{F(s)}{t(s)}\Big]ds \tag{5a}$$

$$\oint_i \frac{F(s)}{t(s)}ds = 2A_i \quad i = 1, ..., n \tag{5b}$$

where $r(s)$ is height of a triangle with the base ds; A_i is the area circumscribed by the contour of the i circuit. The explicit forms of $\omega(s)$ and $F(s)$ for box section are given in Ref.[19].

The displacement components u, v, w representing the deformation of any generic point on the profile section are given with respect to the midsurface displacements $\bar{u}, \bar{v}, \bar{w}$ by the assumption 3.

$$u(s,z,n) = \bar{u}(s,z) \tag{6a}$$

$$v(s,z,n) = \bar{v}(s,z) - n\frac{\partial\bar{u}(s,z)}{\partial s} \tag{6b}$$

$$w(s,z,n) = \bar{w}(s,z) - n\frac{\partial\bar{u}(s,z)}{\partial z} \tag{6c}$$

The strains associated with the small-displacement theory of elasticity are given by

$$\epsilon_s = \bar{\epsilon}_s + n\bar{\kappa}_s \tag{7a}$$

$$\epsilon_z = \bar{\epsilon}_z + n\bar{\kappa}_z \tag{7b}$$

$$\gamma_{sz} = \bar{\gamma}_{sz} + n\bar{\kappa}_{sz} \tag{7c}$$

where

$$\bar{\epsilon}_s = \frac{\partial \bar{v}}{\partial s}; \quad \bar{\epsilon}_z = \frac{\partial \bar{w}}{\partial z} \tag{8a}$$

$$\bar{\kappa}_s = -\frac{\partial^2 \bar{u}}{\partial z^2}; \quad \bar{\kappa}_z = -\frac{\partial^2 \bar{u}}{\partial z^2}; \quad \bar{\kappa}_{sz} = -2\frac{\partial^2 \bar{u}}{\partial s \partial z} \tag{8b}$$

All the other strains are identically zero. In Eq.(8), $\bar{\epsilon}_s$ and $\bar{\kappa}_s$ are assumed to be zero. $\bar{\epsilon}_z$, $\bar{\kappa}_z$ and $\bar{\kappa}_{sz}$ are midsurface axial strain and biaxial curvature of the shell, respectively. The above shell strains can be converted to beam strain components by substituting Eqs.(1), (4) and (6) into Eq.(8) as

$$\bar{\epsilon}_z = \epsilon_z^\circ + x\kappa_y + y\kappa_x + \omega\kappa_\omega \tag{9a}$$

$$\bar{\kappa}_z = \kappa_y \sin\theta - \kappa_x \cos\theta - \kappa_\omega q \tag{9b}$$

$$\bar{\kappa}_{sz} = 2\bar{\chi}_{sz} = \kappa_{sz} \tag{9c}$$

where $\epsilon_z^\circ, \kappa_x, \kappa_y, \kappa_\omega$ and κ_{sz} are axial strain, biaxial curvatures in the x and y direction, warping curvature with respect to the shear center, and twisting curvature in the beam, respectively defined as

$$\epsilon_z^\circ = W' \tag{10a}$$

$$\kappa_x = -V'' \tag{10b}$$

$$\kappa_y = -U'' \tag{10c}$$

$$\kappa_\omega = -\Phi'' \tag{10d}$$

$$\kappa_{sz} = 2\Phi' \tag{10e}$$

The resulting strains can be obtained from Eqs.(7) and (9) as

$$\epsilon_z = \epsilon_z^\circ + (x + n\sin\theta)\kappa_y + (y - n\cos\theta)\kappa_x + (\omega - nq)\kappa_\omega \tag{11a}$$

$$\gamma_{sz} = (n + \frac{F}{2t})\kappa_{sz} \tag{11b}$$

III. VARIATIONAL FORMULATION

The total potential energy of the system can be stated, in its buckled shape, as

$$\Pi = \mathcal{U} + \mathcal{V} \tag{12}$$

where $\mathcal{U}$ is the strain energy

$$\mathcal{U} = \frac{1}{2}\int_v (\sigma_z \epsilon_z + \sigma_{sz}\gamma_{sz}) dv \tag{13}$$

After substituting Eq.(11) into Eq.(13)

$$\mathcal{U} = \frac{1}{2}\int_v \left\{ \sigma_z \Big[\epsilon_z^\circ + (x + n\sin\theta)\kappa_y + (y - n\cos\theta)\kappa_x + (\omega - nq)\kappa_\omega \Big] + \sigma_{sz}(n + \frac{F}{2t})\kappa_{sz} \right\} dv \tag{14}$$

The variation of strain energy can be stated as

$$\delta\mathcal{U} = \int_0^l (N_z \delta\epsilon_z + M_y \delta\kappa_y + M_x \delta\kappa_x + M_\omega \delta\kappa_\omega + M_t \delta\kappa_{sz}) dz \tag{15}$$

where $N_z, M_x, M_y, M_\omega, M_t$ are axial force, bending moments in the x- and y-direction, warping moment (bimoment), and torsional moment with respect to the centroid, respectively, defined by integrating over the cross-sectional area A as

$$N_z = \int_A \sigma_z ds dn \tag{16a}$$

$$M_y = \int_A \sigma_z (x + n\sin\theta) ds dn \tag{16b}$$

$$M_x = \int_A \sigma_z (y - n\cos\theta) ds dn \tag{16c}$$

$$M_\omega = \int_A \sigma_z (\omega - nq) ds dn \tag{16d}$$

$$M_t = \int_A \sigma_{sz} (n + \frac{F}{2t}) ds dn \tag{16e}$$

The potential of in-plane loads $\mathcal{V}$ due to transverse deflection

$$\mathcal{V} = \frac{1}{2}\int_v \overline{\sigma}_z^0 \Big[(u')^2 + (v')^2 \Big] dv \tag{17}$$

where $\overline{\sigma}_z^0$ is the averaged constant in-plane edge axial stress, defined by $\overline{\sigma}_z^0 = P_0/A$. The variation of the potential of in-plane loads at the centroid is expressed by substituting the assumed displacement field into Eq.(17) as

$$\begin{aligned} \delta\mathcal{V} = \int_v \frac{P_0}{A} \Big[& U'\delta U' + V'\delta V' + (q^2 + r^2 + 2rn + n^2)\Phi'\delta\Phi' + (\Phi'\delta U' + U'\delta\Phi')\big[n\cos\theta - (y - y_p)\big] \\ & + (\Phi'\delta V' + V'\delta\Phi')\big[n\cos\theta + (x - x_p)\big] \Big] dv \end{aligned} \tag{18}$$

The kinetic energy of the system is given by

$$\mathcal{T} \;=\; \frac{1}{2}\int_v \rho(\dot{u}^2+\dot{v}^2+\dot{w}^2)dv \tag{19}$$

where ρ is a density.

The variation of the kinetic energy is expressed by substituting the assumed displacement field into Eq.(19) as

$$\begin{aligned}\delta\mathcal{T} \;=\; & \int_v \rho\Big\{\dot{U}\delta\dot{U}+\dot{V}\delta\dot{V}+\dot{W}\delta\dot{W}+(q^2+r^2+2rn+n^2)\dot{\Phi}\delta\dot{\Phi}+(\dot{\Phi}\delta\dot{U}+\dot{U}\delta\dot{\Phi})\Big[n\cos\theta-(y-y_p)\Big] \\ & +\;(\dot{\Phi}\delta\dot{V}+\dot{V}\delta\dot{\Phi})\Big[n\cos\theta+(x-x_p)\Big]\Big\}dv\end{aligned} \tag{20}$$

In order to derive the equations of motion, Hamilton's principle is used

$$\delta\int_{t_1}^{t_2}(\mathcal{T}-\Pi)dt \;=\; 0 \tag{21}$$

Substituting Eqs.(15),(18) and (20) into Eq.(21), the following weak statement is obtained

$$\begin{aligned}0 \;=\; & \int_{t_1}^{t_2}\int_0^l \Big\{m_0\dot{W}\delta\dot{W}+\Big[m_0\dot{U}+(m_c-m_y+m_0y_p)\dot{\Phi}\Big]\delta\dot{U}+\Big[m_0\dot{V}+(m_s+m_x-m_0x_p)\dot{\Phi}\Big]\delta\dot{V} \\ & +\;\Big[(m_c-m_y+m_0y_p)\dot{U}+(m_s+m_x-m_0x_p)\dot{V}+(m_p+m_2+2m_\omega)\dot{\Phi}\Big]\delta\dot{\Phi} \\ & -\;\Big[P_0\big[\delta U'(U'+\Phi'y_p)+\delta V'(V'-\Phi'x_p)+\delta\Phi'(\Phi'\frac{I_p}{A}+U'y_p-V'x_p)\big] \\ & -\;N_z\delta W'+M_y\delta U''+M_x\delta V''+M_\omega\delta\Phi''-2M_t\delta\Phi\Big]\Big\}dzdt\end{aligned} \tag{22}$$

The explicit expressions of inertia coefficients for composite box section are given in Ref.[21].

IV. CONSTITUTIVE EQUATIONS

The constitutive equations of a k^{th} orthotropic lamina in the laminate co-ordinate system of section are given by

$$\left\{\begin{array}{c}\sigma_z\\ \sigma_{sz}\end{array}\right\}^k = \left[\begin{array}{cc}\bar{Q}^*_{11} & \bar{Q}^*_{16}\\ \bar{Q}^*_{16} & \bar{Q}^*_{66}\end{array}\right]^k \left\{\begin{array}{c}\epsilon_z\\ \gamma_{sz}\end{array}\right\} \tag{23}$$

where $\bar{Q}^*_{ij}$ are transformed reduced stiffnesses. The transformed reduced stiffnesses can be calculated from the transformed stiffnesses based on the plane stress assumption and plane strain assumption. More detailed explanation can be found in Ref.[22]

The constitutive equations for bar forces and bar strains are obtained by using Eqs.(11), (16) and (23)

$$\begin{Bmatrix} N_z \\ M_y \\ M_x \\ M_\omega \\ M_t \end{Bmatrix} = \begin{bmatrix} E_{11} & E_{12} & E_{13} & E_{14} & E_{15} \\ & E_{22} & E_{23} & E_{24} & E_{25} \\ & & E_{33} & E_{34} & E_{35} \\ & & & E_{44} & E_{45} \\ \text{sym.} & & & & E_{55} \end{bmatrix} \begin{Bmatrix} \epsilon_z^\circ \\ \kappa_y \\ \kappa_x \\ \kappa_\omega \\ \kappa_{sz} \end{Bmatrix} \tag{24}$$

where E_{ij} are stiffnesses of thin-walled composite beams and given in Ref.[19].

V. GOVERNING EQUATIONS OF MOTION

The governing equations of motion of the present study can be derived by integrating the derivatives of the varied quantities by parts and collecting the coefficients of of $\delta W, \delta U, \delta V$ and $\delta\Phi$

$$N_z' = m_0\ddot{W} \tag{25a}$$

$$M_y'' + P_0\big(U'' + \Phi'' y_p\big) = m_0\ddot{U} + (m_c - m_y + m_0 y_p)\ddot{\Phi} \tag{25b}$$

$$M_x'' + P_0\big(V'' - \Phi'' x_p\big) = m_0\ddot{V} + (m_s + m_x - m_0 x_p)\ddot{\Phi} \tag{25c}$$

$$\begin{aligned} M_\omega'' + 2M_t' + P_0\big(\Phi''\frac{I_p}{A} + U'' y_p - V'' x_p\big) &= (m_c - m_y + m_0 y_p)\ddot{U} \\ &+ (m_s + m_x - m_0 x_p)\ddot{V} + (m_p + m_2 + 2m_\omega)\ddot{\Phi} \end{aligned} \tag{25d}$$

The natural boundary conditions are of the form

$$\delta W \ : \ N_z = P_0 \tag{26a}$$

$$\delta U \ : \ M_y = M_y^0 \tag{26b}$$

$$\delta U' \ : \ M_y' = M_y'^0 \tag{26c}$$

$$\delta V \ : \ M_x = M_x^0 \tag{26d}$$

$$\delta V' \ : \ M_x' = M_x'^0 \tag{26e}$$

$$\delta\Phi \ : \ M_\omega' + 2M_t = M_\omega^{'0} \tag{26f}$$

$$\delta\Phi' \ : \ M_\omega = M_\omega^0 \tag{26g}$$

where $P_0, M_y^{'0}, M_y^0, M_x^{'0}, M_x^0, M_\omega^{'0}$ and M_ω^0 are prescribed values.

Eq.(25) is most general form for flexural-torsional vibration of thin-walled composite beams under a constant axial force, and the dependent variables, W, U, V and Φ are fully coupled. By substituting Eqs.(10) and (24) into Eq.(25),

the explicit form of governing equations of motion can be obtained. If all the coupling effects are neglected and the cross section is symmetrical with respect to both x- and the y-axes, Eq.(25) can be simplified to the uncoupled differential equations as

$$(EA)_{com}W'' = \rho A\ddot{W} \tag{27a}$$

$$-(EI_y)_{com}U^{iv} + P_0U'' = \rho A\ddot{U} \tag{27b}$$

$$-(EI_x)_{com}V^{iv} + P_0V'' = \rho A\ddot{V} \tag{27c}$$

$$-(EI_\omega)_{com}\Phi^{iv} + \Big[(GJ)_{com} + P_0\frac{I_p}{A}\Big]\Phi'' = \rho I_p\ddot{\Phi} \tag{27d}$$

From above equations, $(EA)_{com}$ represents axial rigidity, $(EI_x)_{com}$ and $(EI_y)_{com}$ represent flexural rigidities with respect to x- and y-axis, $(EI_\omega)_{com}$ represents warping rigidity, and $(GJ)_{com}$, represents torsional rigidity of thin-walled composite beams, respectively, written as

$$(EA)_{com} = E_{11} \tag{28a}$$

$$(EI_y)_{com} = E_{22} \tag{28b}$$

$$(EI_x)_{com} = E_{33} \tag{28c}$$

$$(EI_\omega)_{com} = E_{44} \tag{28d}$$

$$(GJ)_{com} = 4E_{55} \tag{28e}$$

It is well known that the three distinct load-frequency interaction curves corresponding to flexural buckling and natural frequencies in the x- and y- direction, and torsional buckling and natural frequency, respectively. They are given by the orthotropy solution for simply supported boundary conditions [23]

$$\omega_{xx_n} = \omega_{x_n}\sqrt{1-\frac{P_0}{P_x}} \tag{29a}$$

$$\omega_{yy_n} = \omega_{y_n}\sqrt{1-\frac{P_0}{P_y}} \tag{29b}$$

$$\omega_{\theta\theta_n} = \omega_{\theta_n}\sqrt{1-\frac{P_0}{P_\theta}} \tag{29c}$$

where $\omega_{x_n}, \omega_{y_n}$ and ω_{θ_n} are corresponding flexural natural frequencies in the x- and y-direction and torsional natural

frequency [4].

$$\omega_{x_n} = \frac{n^2\pi^2}{l^2}\sqrt{\frac{(EI_y)_{com}}{\rho A}} \tag{30a}$$

$$\omega_{y_n} = \frac{n^2\pi^2}{l^2}\sqrt{\frac{(EI_x)_{com}}{\rho A}} \tag{30b}$$

$$\omega_{\theta_n} = \frac{n\pi}{l}\sqrt{\frac{1}{\rho I_p}\Big[\frac{n^2\pi^2}{l^2}(EI_\omega)_{com} + (GJ)_{com}\Big]} \tag{30c}$$

and P_x, P_y and P_θ are also corresponding flexural buckling loads in the x- and y-direction and torsional buckling load [5], respectively.

$$P_x = \frac{\pi^2(EI_y)_{com}}{l^2} \tag{31a}$$

$$P_y = \frac{\pi^2(EI_x)_{com}}{l^2} \tag{31b}$$

$$P_\theta = \frac{A}{I_p}\Big[\frac{\pi^2(EI_\omega)_{com}}{l^2} + (GJ)_{com}\Big] \tag{31c}$$

VI. FINITE ELEMENT FORMULATION

The present theory for thin-walled composite beams described in the previous section was implemented via a displacement based finite element method. The generalized displacements are expressed over each element as a linear combination of the one-dimensional Lagrange interpolation function Ψ_j and Hermite-cubic interpolation function ψ_j associated with node j and the nodal values

$$W = \sum_{j=1}^{n} w_j\Psi_j \tag{32a}$$

$$U = \sum_{j=1}^{n} u_j\psi_j \tag{32b}$$

$$V = \sum_{j=1}^{n} v_j\psi_j \tag{32c}$$

$$\Phi = \sum_{j=1}^{n} \phi_j\psi_j \tag{32d}$$

Substituting these expressions into the weak statement in Eq.(18), the finite element model of a typical element can be expressed as the standard eigenvalue problem

$$([K] - P_0[G] - \omega^2[M])\{\Delta\} = \{0\} \tag{33}$$

where $[K], [G]$ and $[M]$ are the element stiffness matrix, the element geometric stiffness matrix and the element mass matrix, respectively. The explicit forms of $[K], [G]$ and $[M]$ are given in Refs.[19-21].

In Eq.(33), $\{\Delta\}$ is the eigenvector of nodal displacements corresponding to an eigenvalue

$$\{\Delta\} = \{W\ U\ V\ \Phi\}^{\mathrm{T}} \tag{34}$$

VII. NUMERICAL EXAMPLES

A thin-walled composite box beam with length $l = 8$m is considered to investigate the effects of axial force, fiber orientation and modulus ratio on the natural frequencies, load-frequency interaction curves and the corresponding mode shapes. The geometry and stacking sequences of the box section are shown in Fig.2, and the following engineering constants are used

$$E_1/E_2 = 25, G_{12}/E_2 = 0.6, \nu_{12} = 0.25 \tag{35}$$

For convenience, the following nondimensional axial force and natural frequency are used

$$\overline{P} = \frac{Pl^2}{b_1^3 t E_2} \tag{36a}$$

$$\overline{\omega} = \frac{\omega l^2}{b_1}\sqrt{\frac{\rho}{E_2}} \tag{36b}$$

The left and right webs are angle-ply laminates $[\theta/-\theta]$ and $[-\theta/\theta]$ and the flanges laminates are assumed to be unidirectional, (Fig.2a). All the coupling stiffnesses are zero, but E_{25} does not vanish due to unsymmetric stacking sequence of the webs. The lowest three natural frequencies with and without the effect of axial force are given in Table I. The critical buckling loads and the natural frequencies without axial force agree completely with those of previous papers [20,21], as expected. It can be shown from Table I that the change in the natural frequencies due to axial force is significant for all fiber angles. It is noticed that the natural frequencies increase as the axial force changes from compression ($\overline{P} = 0.5 \times P_{cr}$) to tension ($\overline{P} = -0.5 \times P_{cr}$) which reveals that the compressive force has a softening effect on the natural frequencies while the tension force has a stiffening effect. The typical normal mode shapes corresponding to the lowest three natural frequencies with fiber angle $\theta = 30^\circ$ for the case of a compressive axial force ($\overline{P} = 0.5 \times P_{cr}$) are illustrated in Figs.3-5. The mode shapes for other cases of axial force ($\overline{P} = 0$ and $\overline{P} = -0.5 \times P_{cr}$) are similar to the corresponding ones for the case of axial force ($\overline{P} = 0.5 \times P_{cr}$) and are not plotted, although there is a little difference between them. The lowest three interaction diagrams with the fiber angle $\theta = 0^\circ$ and 30° obtained by finite element analysis and the orthotropy solution, which neglects the coupling effects of E_{25} from Eqs.(29a)-(29c) are plotted in Figs.6 and 7. For unidirectional fiber direction (Fig.6), the smallest

curve exactly corresponds to the first flexural in x-direction and the larger ones correspond to the first flexural in y-direction and the second flexural in x-direction of the orthotropy solution, respectively. However, as the fiber angle and axial compressive force increase, this order is changing. It can be explained partly by the interaction diagram between flexural buckling and natural frequency with the fiber angle $\theta = 30^\circ$ in Fig.7. When the beam is subjected to small axial compressive force, the vibration mode 1 and 2 are the first flexural x- and y-direction (Figs.3 and 4). Thus, the othotropy solution and the finite element analysis are identical. It is from Fig.5 that the vibration mode 3 exhibits double coupling (the second flexural mode in x-direction and torsional mode). Due to the small coupling stiffnesses E_{25}, this mode becomes predominantly the second flexural x-direction mode, with a little contribution from torsion. Therefore, the results by the finite element analysis ($w_3 - P_3$) and orthotropy solution ($w_{x_2} - P_{x_2}$) are nearly identical in Fig.7. It is indicated that the simple orthotropy solution is sufficiently accurate for this stacking sequence. Characteristic of load-frequency interaction curves is that the value of the axial force for which the natural frequency vanishes constitutes the critical buckling load. Thus, for $\theta = 30^\circ$, the first flexural buckling in minor axis occurs at $\overline{P} = 13.88$. Therefore, the lowest branch vanishes when $\overline{P}$ is slightly over this value. As axial force increases, two interaction curves $w_{y_1} - P_{y_1}$ and $w_{x_2} - P_{x_2}$ intersect at $\overline{P} = 48.10$, thus, after this value, vibration mode 2 and 3 change each other. Finally, the second and third branch will also disappear when $\overline{P}$ is slightly over 54.53 and 73.16, respectively. Figs.6 and 7 explain the duality between flexural buckling and natural frequency. A comprehensive three dimensional interaction diagram of natural frequency, axial compression and fiber angle is plotted in Fig.8. Three groups of curves are observed. The smallest group is for the first flexural mode in x-direction and the larger ones are for the first flexural mode in y-direction and flexural-torsional coupled mode, respectively.

The next example is the same as before except that in this case, the top flange and the left web laminates are $[\theta_2]$, while the bottom flange and right web laminates are unidirectional, (Fig.2b). For this lay-up, the coupling stiffnesses $E_{14}, E_{15}, E_{23}, E_{25}$ and E_{35} become no more negligibly small. Major effects of compressive axial force on the natural frequencies are again seen in Table II. Three dimensional interaction diagram between flexural-torsional buckling and natural frequency with respect to the fiber angle change is shown in Fig.9. Similar phenomena as the previous example can be observed except that in this case all three groups are flexural-torsional coupled mode. The interaction diagram between flexural-torsional buckling and natural frequency by the finite element analysis and orthotropy solution with the fiber angle $\theta = 30^\circ$ and 60° are displayed in in Figs.10 and 11. It can be remarked again that the natural frequencies decrease with the increase of compressive axial forces, and the decrease becomes more quickly when axial forces are close to flexural-torsional buckling loads. For $\theta = 60^\circ$, at about $\overline{P}$= 7.92, 31.28 and 47.11, respectively, the

natural frequencies become zero which implies that at these loads, flexural-torsional bucklings occur as a degenerate case of natural vibration at zero frequency. As the fiber angle and compressive axial force increases, the orthotropy solution and the finite element analysis solution show significantly discrepancy (Figs.10 and 11). The typical normal mode shapes corresponding to the lowest three natural frequencies with fiber angle $\theta = 60^\circ$ for the case of compressive axial force ($\overline{P} = 0.5 \times P_{cr}$) are illustrated in Figs.12-14. Relative measures of flexural displacements and torsional rotation show that all the modes are triply coupled mode (flexural mode in the x- and y-directions and torsional mode). That is, the orthotropy solution is no longer valid for unsymmetrically laminated beams, and triply coupled flexural-torsional vibration should be considered even for a doubly symmetric cross-section.

Finally, the effects of modulus ratio (E_1/E_2) on the first five natural frequencies of a cantilever thin-walled composite beam under a compressive axial force ($\overline{P} = 0.5 \times P_{cr}$) are investigated. The stacking sequence of the flanges and webs are $[0/90]_s$, (Fig.2c). For this lay-up, all the coupling stiffnesses vanish and thus, the three distinct vibration mode, flexural vibration in the x- and y-direction and torsional vibration are identified. It is observed from Fig.15 that the natural frequencies $\omega_{xx_1}, \omega_{yy_1}, \omega_{xx_2}$ and ω_{yy_2} increase with increasing orthotropy (E_1/E_2). However, torsional natural frequency is almost invariant and well above the other three types of natural frequencies, i.e. $\omega_{xx_1}, \omega_{yy_1}$ and ω_{xx_2}. It can be explained from Eqs.(29c) and (30c) that torsional frequency is dominated by torsional rigidity rather than warping rigidity. Moreover, effects of warping is negligibly small for box section. As ratio of (E_1/E_2) increases, the order of the second flexural mode in the y-direction, the torsional mode change each other.

VIII. CONCLUDING REMARKS

An analytical model is developed to study the flexural-torsional coupled vibration of thin-walled composite beams with arbitrary lay-ups under a constant axial force. This model is capable of predicting accurately the natural frequencies and load-frequency interaction curves as well as corresponding vibration mode shapes for various. To formulate the problem, a one-dimensional displacement-based finite element method is employed. All of the possible vibration modes including the flexural mode in the x- and y-direction and the torsional mode, and fully coupled flexural-torsional mode are included in the analysis. The present model is found to be appropriate and efficient in analyzing free vibration problem of thin-walled composite beams under a constant axial force.

Acknowledgments

The support of the research reported here by a grant (code #06 R&D B03) from Cutting-edge Urban Development Program funded by the Ministry of Land, Transport and Maritime Affairs of Korea government is gratefully acknowledged. The authors also would like to thank the anonymous reviewers for their suggestions in improving the standard of the manuscript.

References

[1] Vlasov VZ. Thin Walled Elastic Beams, Israel Program for Scientific Translation, Jerusalem, 1961.

[2] Gjelsvik A. The theory of thin-walled bars, New York: John Wiley and Sons Inc., 1981.

[3] Timoshenko SP and Gere JM. Theory of elastic stability. New York: McGraw-Hill, 1963.

[4] Timoshenko SP, Young DH and Weaver W. Vibration problems in engineering. New York: Wiley, 1974.

[5] Trahair NS. Flexural-torsional buckling of structures. London: CRC Press, 1993.

[6] Banerjee JR and Williams FW. Exact dynamic stiffness matrix for composite Timoshenko beams with applications. J Sound Vib 1996; 194(4):573-585.

[7] Banerjee JR. Free vibration of axially loaded composite Timoshenko beams using the dynamic stiffness matrix method. Comput Struct 1998;69(2):197-208.

[8] Li J, Shen R and Jin X. Bending-torsional coupled dynamic response of axially loaded composite Timosenko thin-walled beam with closed cross-section. Compos Struct 2004;64(1):23-35.

[9] Li J and Jin X. Response of flexure-torsion coupled composite thin-walled beams with closed cross-sections to random loads. Mech Res Commun 2005; 32(1):25-41.

[10] Li J, Wu G, Shen R and Hua H. Stochastic bending-torsion coupled response of axially loaded slender composite thin-walled beams with closed cross-sections. Int J Mech Sci 2005; 47(1):134-155.

[11] Li J, Hua H and Shen R. Dynamic stiffness analysis for free vibrations of axially loaded laminated composite beams. Compos Struct 2008; 84(1):87-98.

[12] Kaya MO and Ozgumus OO. Flexural-torsional-coupled vibration analysis of axially loaded closed-section composite Timoshenko beam by using DTM. J Sound Vib 2007; 306(3-5):495-506.

[13] Bank LC and Kao CH. Dynamic Response of Thin-Walled Composite Material Timoshenko Beams. J Energ Resour 1990; 112:149-154.

[14] Song O, Jeong NH and Librescu L. Vibration and stability of pretwisted spinning thin-walled composite beams featuring bending-bending elastic coupling. J Sound Vib 2000; 237(3):513-533.

[15] Cortinez VH and Piovan MT. Vibration and buckling of composite thin-walled beams with shear deformability. J Sound Vib 2002; 258(4-5):701-723.

[16] Machado SP and Cortinez VH. Free vibration of thin-walled composite beams with static initial stresses and deformations. Eng Struct 2007; 29(3):372-382.

[17] Machado SP, Filipich CP and Cortinez VH. Parametric vibration of thin-walled composite beams with shear deformation. J Sound Vib 2007;305(4-5):563-581.

[18] Sapountzakis EJ and Tsiatas GC. Flexural - Torsional Buckling and Vibration Analysis of Composite Beams. Comput Mater Con 2007; 6(2), 103-115.

[19] Vo TP and Lee J. Flexural-torsional behavior of thin-walled closed-section composite box beams. Eng Struct 2007; 29(8):1774-1782.

[20] Vo TP and Lee J. Flexural-torsional buckling of thin-walled composite box beams. Thin-Walled Struct 2007; 45(9):790-798.

[21] Vo TP and Lee J. Free vibration of thin-walled composite box beams. Compos Struct 2008; 84(1):11-20.

[22] Jones RM. Mechanics of composite materials, New York: Hemisphere Publishing Corp., 1975.

[23] Mohri F, Azrar L and Potier-Ferry M. Vibration analysis of buckled thin-walled beams with open sections. J Sound Vib 2004; 275(1-2):434-446.

CAPTIONS OF TABLES

Table I: Effect of axial force on the first three natural frequencies with respect to the fiber angle change in the webs of a simply supported composite beam.

Table II: Effect of axial force on the first three natural frequencies with respect to the fiber angle change in the left web and top flange of a simply supported composite beam.

CAPTIONS OF FIGURES

Figure 1: Definition of coordinates in thin-walled closed sections.

Figure 2: Geometry and stacking sequences of thin-walled composite box beam.

Figure 3: Mode shapes of the flexural and torsional components for the first mode $\omega_1 = 4.721$ with the fiber angle 30° in the webs of a simply supported composite beam under a compressive axial force $\overline{P} = 0.5P_{cr}$.

Figure 4: Mode shapes of the flexural and torsional components for the second mode $\omega_2 = 14.750$ with the fiber angle 30° in the webs of a simply supported composite beam under a compressive axial force $\overline{P} = 0.5P_{cr}$.

Figure 5: Mode shapes of the flexural and torsional components for the third mode $\omega_3 = 24.965$ with the fiber angle 30° in the webs of a simply supported composite beam under a compressive axial force $\overline{P} = 0.5P_{cr}$.

Figure 6: Effect of axial force on the first three natural frequencies with the fiber angle 0° in the webs of a simply supported composite beam.

Figure 7: Effect of axial force on the first three natural frequencies with the fiber angle 30° in the webs of a simply supported composite beam.

Figure 8: Three dimensional interaction diagram between between axial force and the first three natural frequencies with respect to the fiber angle change in the webs of a simply supported composite beam.

Figure 9: Three dimensional interaction diagram between axial force and the first three natural frequencies with respect to the fiber angle change in the left web and top flange of a simply supported composite beam.

Figure 10: Effect of axial force on the first three natural frequencies with the fiber angle 30° in the left web and top flange of a simply supported composite beam.

Figure 11: Effect of axial force on the first three natural frequencies with the fiber angle 60° in the left web and top flange of a simply supported composite beam.

Figure 12: Mode shapes of the flexural and torsional components for the first mode $\omega_1 = 3.609$ of a simply supported composite beam under a compressive axial force $\overline{P} = 0.5P_{cr}$ with the fiber angle 60° in the top flange and the left web.

Figure 13: Mode shapes of the flexural and torsional components for the second mode $\omega_2 = 11.892$ with the fiber angle 60° in the top flange and the left web of a simply supported composite beam under a compressive axial force $\overline{P} = 0.5P_{cr}$.

Figure 14: Mode shapes of the flexural and torsional components for the third mode $\omega_3 = 18.955$ with the fiber angle 60° in the top flange and the left web of a simply supported composite beam under a compressive axial force

$\overline{P} = 0.5P_{cr}$.

Figure 15: Variation of the first five natural frequencies with respect to modulus ratio change of a cantilever composite beam under a compressive axial force $\overline{P} = 0.5P_{cr}$.

TABLE I Effect of axial force on the first three natural frequencies with respect to the fiber angle change in the webs of a simply supported composite beam.

Fiber	Buckling	$\overline{P} = 0.5 \times P_{cr}$ (compression)			$\overline{P}$=0 (no axial force)			$\overline{P} = -0.5 \times P_{cr}$ (tension)		
angle	loads (P_{cr})	w_1	w_2	w_3	w_1	w_2	w_3	w_1	w_2	w_3
0	36.009	7.696	16.704	40.725	10.884	18.392	43.536	13.330	19.937	46.177
15	29.245	6.936	16.142	36.668	9.809	17.569	39.204	12.013	18.889	41.586
30	13.549	4.721	14.750	24.965	6.677	15.487	26.691	8.177	16.191	28.312
45	7.858	3.595	14.211	19.021	5.084	14.659	20.334	6.227	15.094	21.568
60	6.670	3.312	14.097	17.527	4.685	14.481	18.738	5.737	14.855	19.874
75	6.419	3.249	14.072	17.194	4.595	14.442	18.381	5.628	14.803	19.496
90	6.375	3.238	14.068	17.136	4.580	14.436	18.319	5.609	14.795	19.430

TABLE II Effect of axial force on the first three natural frequencies with respect to the fiber angle change in the left web and top flange of a simply supported composite beam.

Fiber	Buckling	$\overline{P} = 0.5 \times P_{cr}$ (compression)			$\overline{P}$=0 (no axial force)			$\overline{P} = -0.5 \times P_{cr}$ (tension)		
angle	loads (P_{cr})	w_1	w_2	w_3	w_1	w_2	w_3	w_1	w_2	w_3
0	36.009	7.696	16.704	40.725	10.884	18.392	43.536	13.330	19.937	46.177
15	30.211	7.054	15.678	32.717	9.976	17.191	35.542	12.218	18.582	38.154
30	17.016	5.295	13.099	24.088	7.488	14.129	26.285	9.170	15.089	28.311
45	9.899	4.036	12.093	20.324	5.707	12.749	21.864	6.990	13.373	23.302
60	7.918	3.609	11.892	18.955	5.104	12.427	20.282	6.251	12.941	21.528
75	7.454	3.502	11.846	18.517	4.952	12.353	19.797	6.065	12.839	20.999
90	7.370	3.482	11.837	18.424	4.924	12.338	19.696	6.031	12.820	20.891

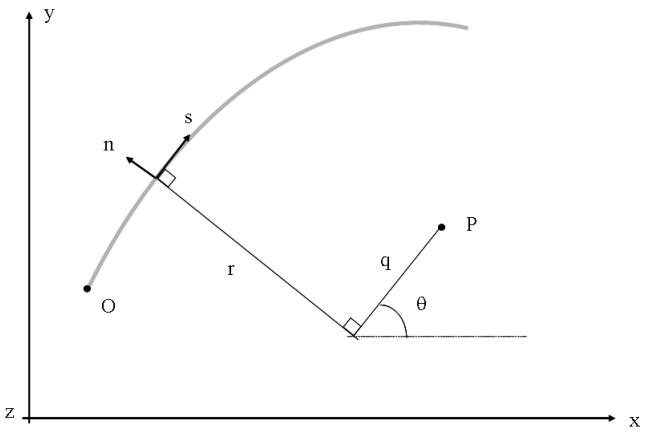

FIG. 1 Definition of coordinates in thin-walled closed sections

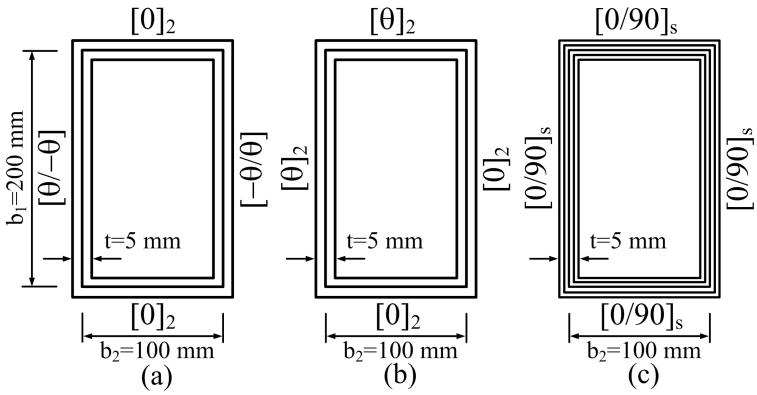

FIG. 2 Geometry and stacking sequences of thin-walled composite box beam.

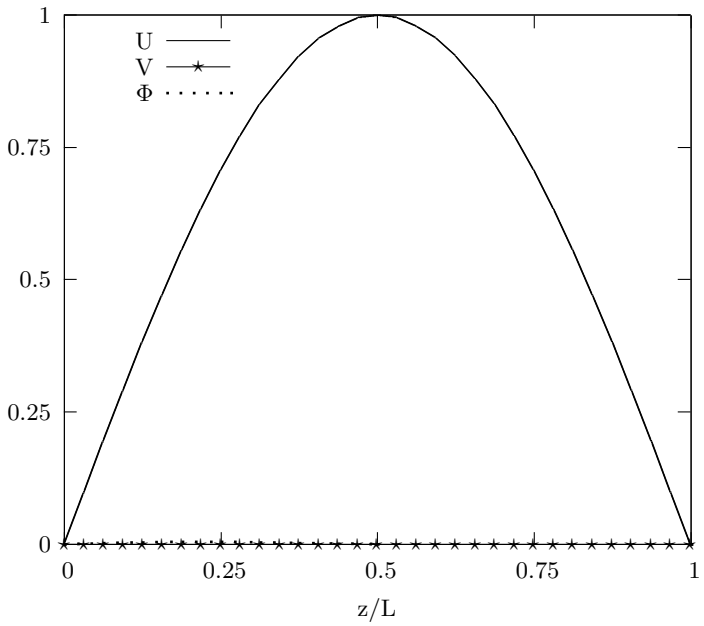

FIG. 3 Mode shapes of the flexural and torsional components for the first mode $\omega_1 = 4.721$ with the fiber angle 30° in the webs of a simply supported composite beam under a compressive axial force $\overline{P} = 0.5P_{cr}$.

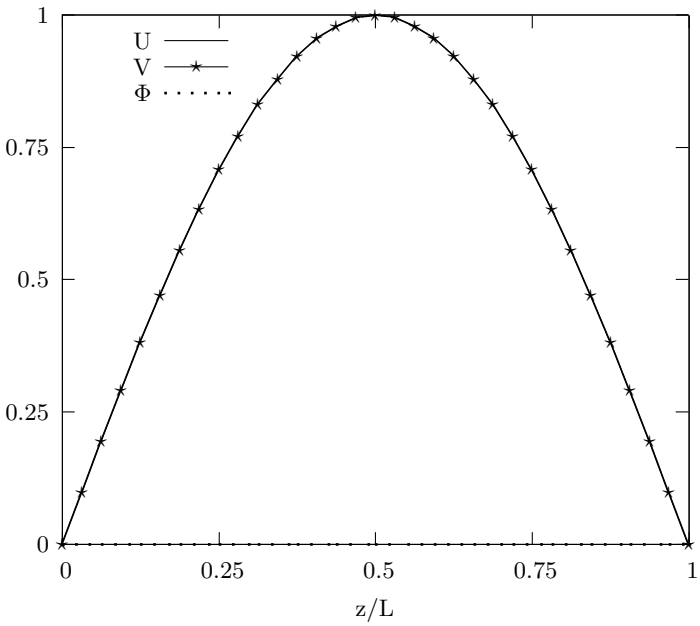

FIG. 4 Mode shapes of the flexural and torsional components for the second mode $\omega_2 = 14.750$ with the fiber angle 30° in the webs of a simply supported composite beam under a compressive axial force $\overline{P} = 0.5P_{cr}$.

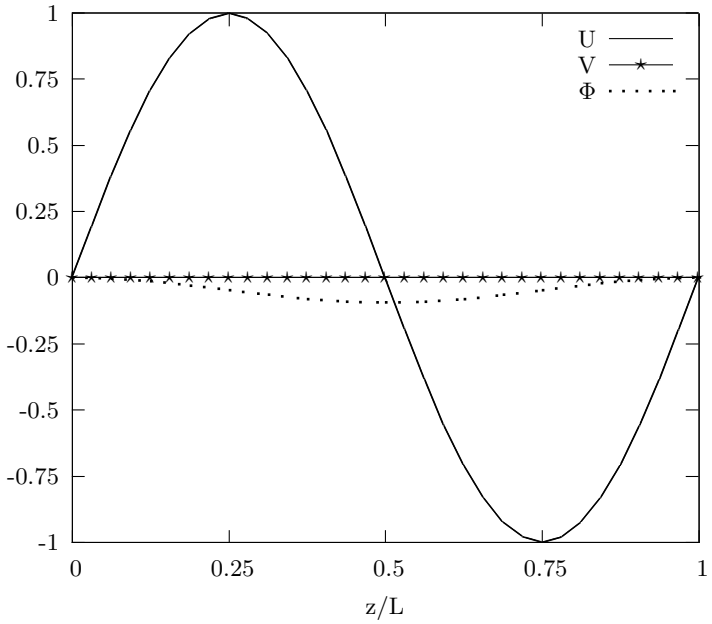

FIG. 5 Mode shapes of the flexural and torsional components for the third mode $\omega_3 = 24.965$ with the fiber angle 30° in the webs of a simply supported composite beam under a compressive axial force $\overline{P} = 0.5P_{cr}$.

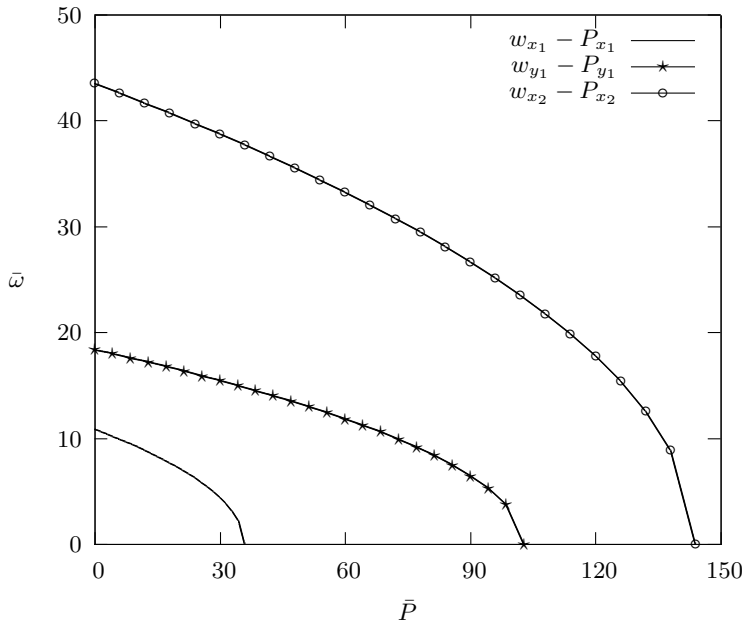

FIG. 6 Effect of axial force on the first three natural frequencies with the fiber angle 0° in the webs of a simply supported composite beam.

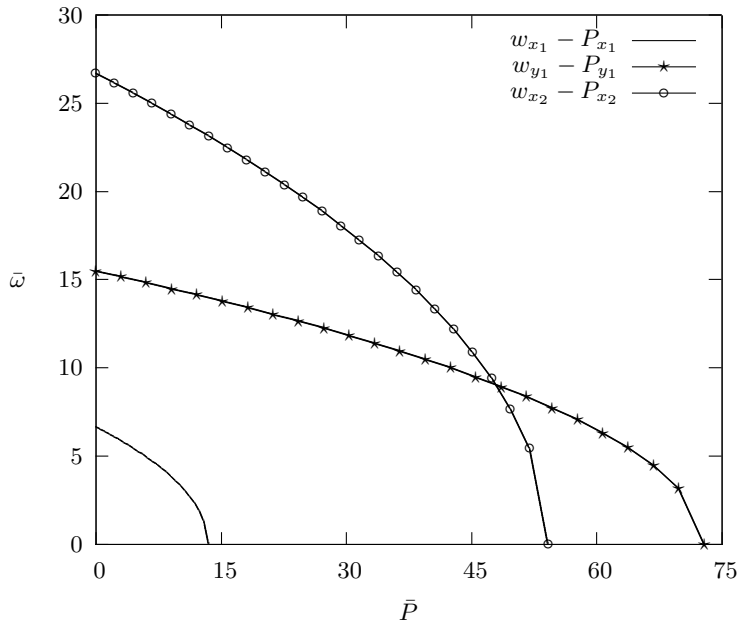

FIG. 7 Effect of axial force on the first three natural frequencies with the fiber angle 30° in the webs of a simply supported composite beam.

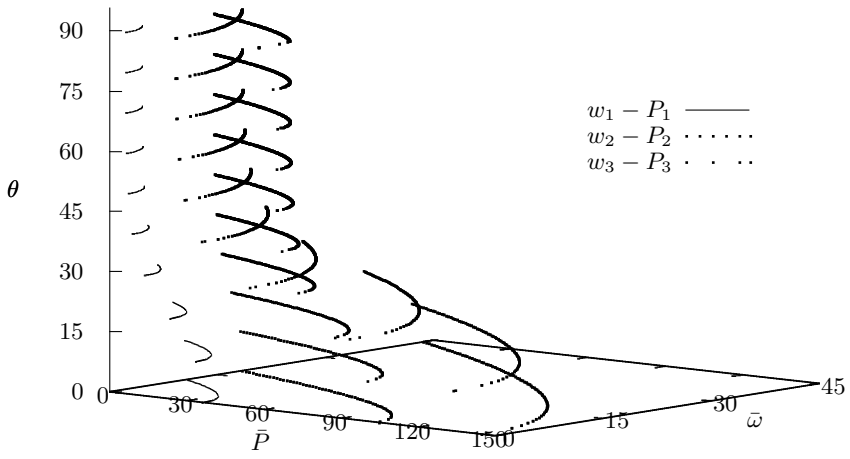

FIG. 8 Three dimensional interaction diagram between between axial force and the first three natural frequencies with respect to the fiber angle change in the webs of a simply supported composite beam.

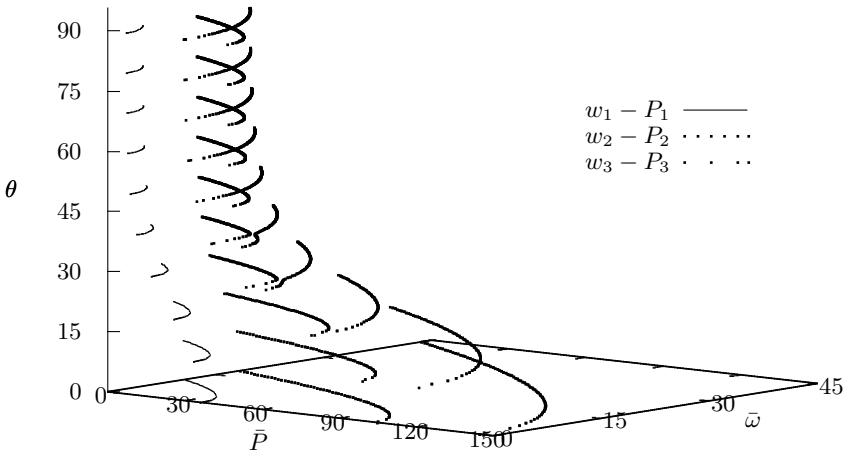

FIG. 9 Three dimensional interaction diagram between axial force and the first three natural frequencies with respect to the fiber angle change in the left web and top flange of a simply supported composite beam.

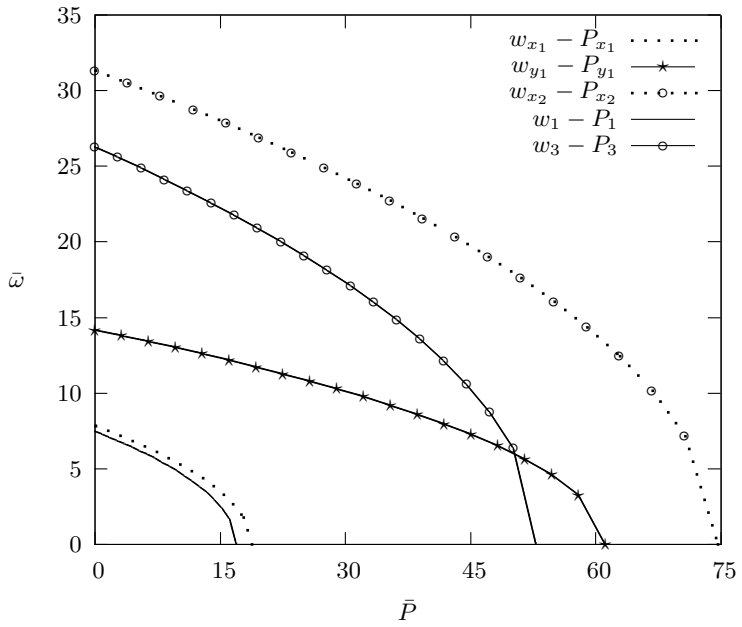

FIG. 10 Effect of axial force on the first three natural frequencies with the fiber angle 30° in the left web and top flange of a simply supported composite beam.

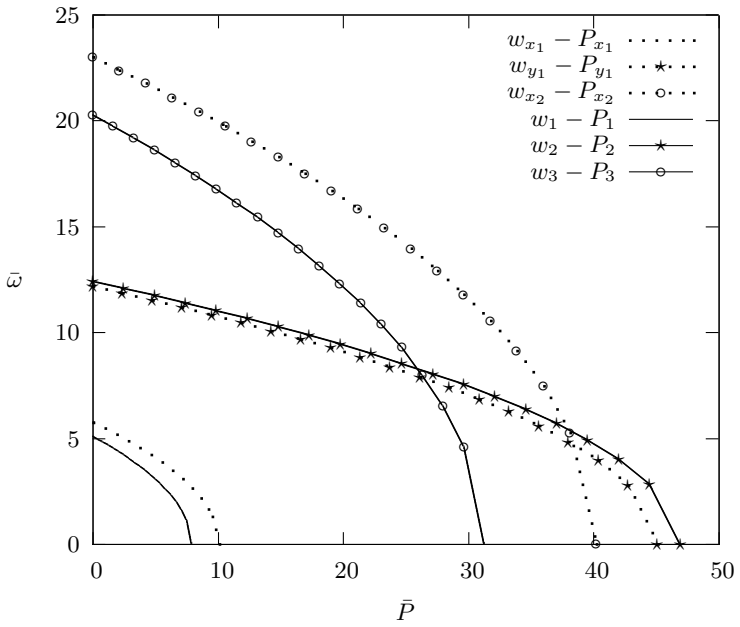

FIG. 11 Effect of axial force on the first three natural frequencies with the fiber angle 60° in the left web and top flange of a simply supported composite beam.

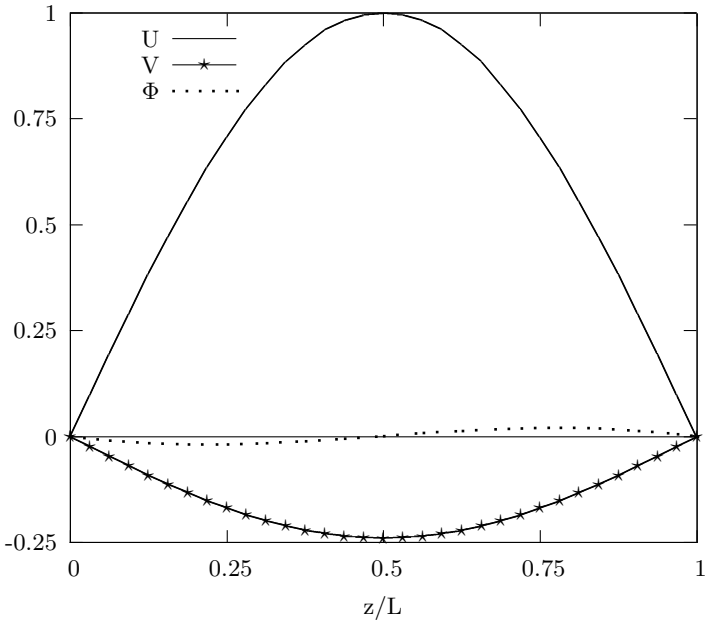

FIG. 12 Mode shapes of the flexural and torsional components for the first mode $\omega_1 = 3.609$ with the fiber angle 60° in the top flange and the left web of a simply supported composite beam under a compressive axial force $\overline{P} = 0.5P_{cr}$.

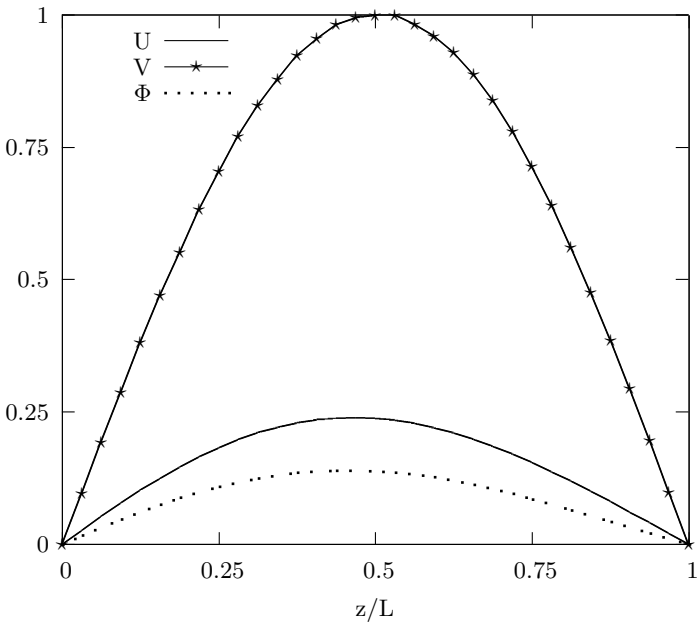

FIG. 13 Mode shapes of the flexural and torsional components for the second mode $\omega_2 = 11.892$ with the fiber angle 60° in the top flange and the left web of a simply supported composite beam under a compressive axial force $\overline{P} = 0.5P_{cr}$.

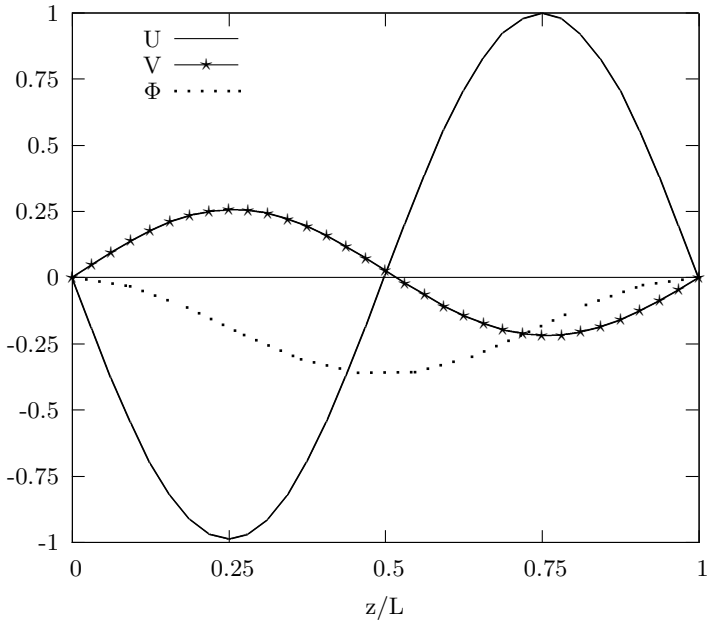

FIG. 14 Mode shapes of the flexural and torsional components for the third mode $\omega_3 = 18.955$ with the fiber angle 60° in the top flange and the left web of a simply supported composite beam under a compressive axial force $\overline{P} = 0.5P_{cr}$.

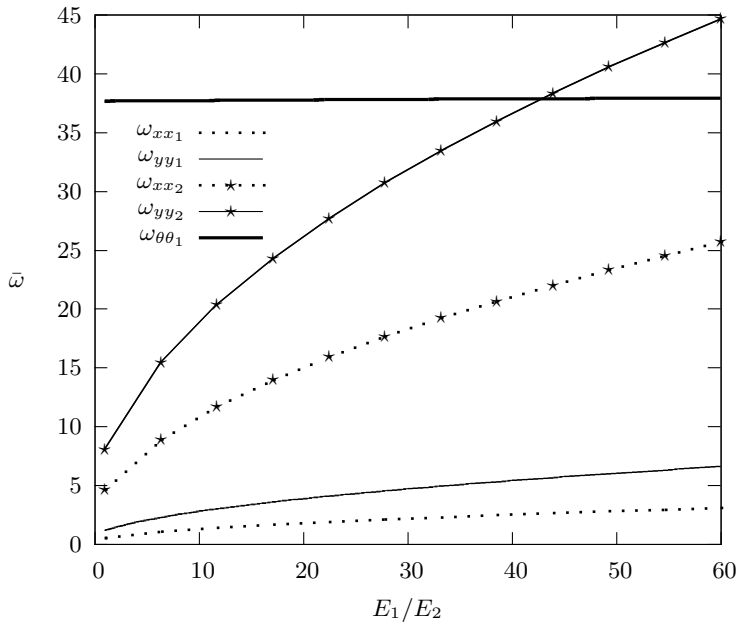

FIG. 15 Variation of the first five natural frequencies natural frequencies with respect to modulus ratio change of a cantilever composite beam under a compressive axial force $\overline{P} = 0.5P_{cr}$.